Cranked Nilsson-Strutinsky model applied to high spin states in ^{22,23}Na: Systematics of rotational isomers and band terminations in the $A = 20$–26 region

D. M. Headly and R. K. Sheline
Departments of Chemistry and Physics, Florida State University, Tallahassee, Florida 32306

Ingemar Ragnarsson
Department of Mathematical Physics, Lund Institute of Technology, Lund, Sweden
(Received 4 May 1993)

Previously proposed high spin states in ^{22,23}Na are compared with calculations from the cranked Nilsson model including Strutinsky renormalization. High K rotational isomers are proposed for $I^\pi = 6^-$ in ^{22}Na and $11/2^+$, $13/2^+$, and possibly $15/2^+$ in ^{23}Na. The positive parity yrast sequences in these two nuclei are analyzed in terms of the change from collective to single particle behavior at $I = 9$ (^{22}Na) and $17/2$ (^{23}Na). The systematics of band terminations in eight nuclei between ^{20}Ne and ^{26}Mg shows that I^{max} or $I^{max}-1$ has tentatively been reached in six of these eight nuclei, where I^{max} is the maximum possible *sd* shell spin for the given nucleus.

PACS number(s): 21.60.Ev, 21.10.Re, 27.30.+t

I. INTRODUCTION

The cranked Nilsson model including Strutinsky renormalization (CNSM) without pairing has been useful in interpreting the spectra of *sd*-shell nuclei at high spin. In particular, the model has provided an explanation of certain states throughout this mass region in terms of band terminations (^{16}O, ^{20,22}Ne, ^{24}Mg), shape coexistence (prolate and oblate in ^{28}Si), rotational coexistence with axial symmetry ($\gamma = -120°$ and $\gamma = 0°$ in $^{24-26}$Mg) or with triaxial shapes ($\gamma = 30°$–$40°$ coexisting with $-30°$ to $-40°$ in ^{16}O), and highly deformed molecular resonances ($\epsilon = 1.1$, $\gamma = 40°$ in ^{24}Mg) [1–4]. Vermeer [5] has recently identified the yrast 6^- state in ^{22}Na and compared the properties of this 6_1^- state (6958 keV) and the 6_2^- state (7413 keV) with the $11/2_1^+$ and $11/2_2^+$ states in ^{23}Na, suggesting that the 6_1^- and $11/2_2^+$ are K isomers. While the shell model calculations used for states in ^{22,23}Na do well at reproducing energy levels and branching ratios for these possible aligned states, they are unable both to give any intuitive picture of these states in terms of deformation, ϵ_2 and γ, and to explain why such high K states are favored in energy relative to collective states of like spin. Therefore, we have looked at ^{22,23}Na using the CNSM to search for possible rotational isomers (or K isomers) and to investigate how the parameters used thus far for *sd*-shell nuclei can reproduce the spectra of Na nuclei. A summary of the current status of band terminations in *sd*-shell nuclei between $A = 20$ and 26 is also presented.

Within a given axially deformed nucleus, we define the term "rotational isomers" as two (or more) states of the same spin and similar gross shape but with the spin vector in different directions. In the *sd* shell only prolate isomers have been proposed. These correspond to collective rotation with the spin vector perpendicular to the symmetry axis and to aligned coupling, along the symmetry axis, of the single-particle spins of the unpaired valence nucleons, respectively. The aligned isomers, often referred to as "rotating around the symmetry axis," do not necessarily possess a long lifetime (e.g., nanoseconds or longer) although this is true in rare earth nuclei and would be true in general for ideal cases.

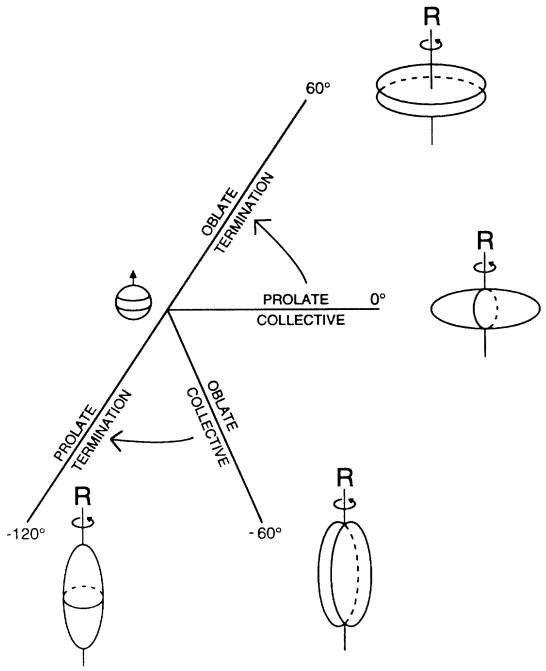

FIG. 1. Polar plot of quadrupole deformed nuclear shapes rotating around the x axis, illustrating the transition through γ from collective oblate shapes ($\gamma = -60°$) at the end of a shell to prolate particle hole alignment at $\gamma = -120°$, contrasted with the experimentally observed changes from prolate collective shapes at $\gamma = 0°$ to oblate noncollective terminations with $\gamma = 60°$at the beginning of shells.

The majority of observed rotational bandheads in the *sd* shell are thought to be prolate (the $11/2_1^+$ state in ^{25}Mg and the ^{28}Si ground state are two exceptions) and hence in the CNSM these bandheads appear at $\gamma = -120°$. The collective bands built on these bandheads through rotation perpendicular to the symmetry axis are then found at γ near 0° where thus, in the standard CNSM, the bandhead spin contribution to the total spin is neglected. With increasing spin, the matter distribution tends to become symmetric around the rotation axis, i.e., a tendency towards triaxial shape and finally a termination for oblate shape ($\gamma = 60°$). If we consider holes instead of particles, oblate collective bands ($\gamma = -60°$) will evolve through decreasing γ values and terminate at $\gamma = -120°$. Thus, in the terminating state, a few valence particles rotating around the equator give rise to an oblate shape ($\gamma = 60°$) while a few holes rotating around the equator lead to a prolate shape ($\gamma = -120°$). Figure 1 gives a pictorial representation of these shapes and rotation axes in the ϵ,γ plane. In practice no bands have been traced from −60° to −120° although in ^{24,25}Mg and ^{28}Si such bands have been predicted in calculations [2–4].

II. MODEL CONSIDERATIONS

The version of the CNSM used here is the same as that described elsewhere [2–4, 6] and we refer the reader to these papers for details of the model. In the present work, we have used standard values [6] for the parameters κ,μ except in the N=2 shell where $\kappa = 0.105$, $\mu = 0.15$ were used. These values can be compared to earlier *sd*-shell calculations [4,6] in which κ,μ=0.08, 0.0 for N=0–2. The important parameter change in the present work is that $\mu(N=2)$ is chosen $\neq 0$. This change produces a lowering of the $d_{5/2}$ subshell energy relative to that of $s_{1/2}$; see Fig. 2. The older values produced a crossing at $\epsilon \sim 0.2$ of the [211]1/2 and [202]5/2 orbitals for prolate shapes, yielding an incorrect $1/2^+$ ground state for ^{25}Mg. The present analysis of ^{22}Na is the first study of an odd-odd light nuclide with the CNSM. In this method, at a specific deformation, proton and neutron single-particle energies and spins are simply added with no special symmetrization. The resulting energies are normalized according to the Strutinsky prescription and then the minimum at fixed spin over different deformations is searched for. In an odd-odd nucleus, a more realistic basis function would be a product of the type $\Psi_p\Psi_n$ so that symmetric and antisymmetric combinations of these functions would be able to yield two states for given spins and configurations ($K \neq 0$) rather than one as in the present calculations. Other limitations are the one-dimensional cranking approximation $I = I_x$, and the exclusion of pairing (which may be significant at low spins) and *n*-*p* interactions. Hence, a detailed comparison of experiment and theory is not feasible. Instead, we will focus on the competition between aligned and collective configurations (at higher spins) and look at overall trends within the yrast bands in ^{22,23}Na. It will be seen that the CNSM can still yield important details concerning the nature of angular momenta coupling and deformation of high spin states in light nuclei.

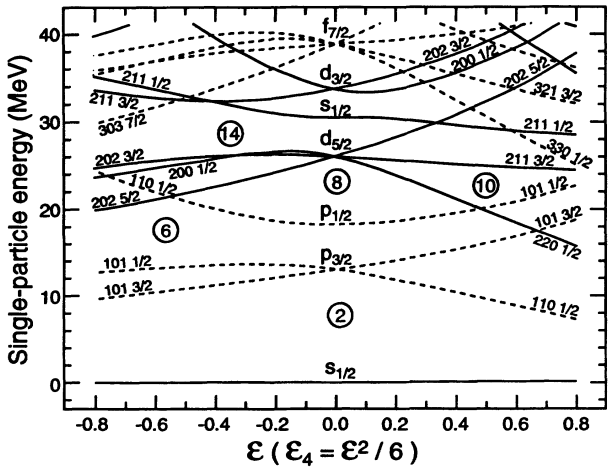

FIG. 2. Static Nilsson model single-particle orbitals (no cranking) for the *p* and *sd* shells, with both quadrupole and hexadecapole (ϵ_4) deformations on the abscissa. Closed (sub)shells are labeled as encircled numbers.

III. COMPARISON OF EXPERIMENT AND THEORY

A. ^{22}Na

In the ground state the odd proton and neutron both occupy the [211]3/2 Nilsson orbital (see Fig. 2). For odd-odd, $N = Z$ nuclei such as this, isospin considerations produce three low lying positive parity bands [7]. Specifically, the odd particles couple to (K^π, T) = (3^+, 0), I = 3, 4, 5, . . . ; (0^+, 0), I = 1, 3, 5, . . . ; and (0^+, 1), I=0, 2, 4 , ... Experimentally the bandheads are at 0, 583, and 657 keV, respectively [8]. We will not look at these bands in detail as explained above.

1. The 6⁻ levels at 6958 and 7413 keV

A 6^- level at 7.474 MeV was first tentatively suggested by Rivet *et al.* [9] using the ^{20}Ne (α, d) reaction. They assigned the configuration as $(d_{5/2}f_{7/2})_{6^-}$. Two more (α, d) experiments [10, 11] also tentatively identified such a state, at 7.46 MeV. R.M. Freeman *et al.* [12] suggested instead that this level was a member of the K^π=1^- band beginning at 2212 keV, based only on rotational energy systematics. Vermeer [5] observed a 7.413 MeV, 6^- state and also placed it in the K^π=1^- band, associating it with the 7.46 MeV state mentioned above. Figure 3 shows the decays of the 6_1^- (6958 keV) and 6_2^- (7413 keV) states and their lifetimes. On the basis of these decay schemes, we have placed 6_2^- at 7413 keV in the K^π=1^- band. The 6_1^- state at 6958 keV has a relatively long half-life and gamma decay outside of the K^π=1^- band, with $B(E2)$ values for transitions from the lowest calculated 6^- state to the 4^- and 5^- states roughly 0.1 W.u. [5], compared to an experimental $B(E2)$ of 16±4 Wu for the $6_2 \rightarrow 4_1$

transition. Furthermore, the 6_2^- level better fits into the $J(J+1)$ energy sequence of the $K^\pi=1^-$ band. These factors suggest $K^\pi=6^-$ for the 6_1^- state, analogous to the situations in $^{24-26}$Mg where noncollective yrast high spin states successfully compete in energy with collective states of like spin [3].

A low lying prolate $K^\pi=6^-$ state of negative parity in ^{22}Na can arise by exciting either a proton or neutron from the p shell ([101]1/2 or [101]3/2 Nilsson orbitals; see Fig. 2). The alternative possibility to put a proton or neutron into the fp shell ([330]1/2) is not favored as shown below. Specifically, the 6^- p-shell hole configuration would be formed from the excitation of a proton or neutron from $[101]^-1/2$ to [202]5/2 relative to the ground state configuration with one proton and one neutron in [211]3/2. This configuration will generate two 6^- states, corresponding to the symmetric and antisymmetric combinations of wave functions with proton and neutron excitations, respectively. For the lower spin states of negative parity, the experimental consensus is that the $K^\pi=1^-$ band beginning at 2212 keV is due to a p-shell hole [13, 14], [211]3/2−[101]1/2, while the corresponding parallel coupled $K^\pi=2^-$, $T=0$ bandhead is experimentally observed at 4583 keV [14]. The lowest fp-shell excitation is tentatively experimentally observed at 6326 keV, with either 1^- or 2^- ([211]3/2 ± [330]1/2) [8, 14].

Figure 4 shows potential energy surfaces (PES's) for the 6^- states in ^{22}Na based on the configuration with (a) a one-neutron p-shell hole and (b) a one-proton fp-shell excitation. In the former, the unpaired $N=1$ neutron has signature $\alpha_\nu=1/2$, coupled to an unpaired $N=2$ proton with $\alpha_\pi=-1/2$. The total signature is then $\alpha_{\rm tot}=0$ with even spins resulting. In (b), the excited proton in $N=3$ has $\alpha_\pi=-1/2$, coupled to an $N=2$ unpaired neutron with $\alpha_\nu=1/2$ again leading to $\alpha_{\rm tot}=0$. Since, in our calculations, it is possible to distinguish protons from neutrons, the PES's for the reverse combinations of $\alpha_\pi+\alpha_\nu$ are slightly different. The general features of competing collective and noncollective minima are nonetheless represented in our picture. For the p-shell hole PES in (a) we notice that the yrast configuration, at 11.9 MeV, lies at $(\epsilon,\gamma)=0.3, -120°$, i.e., a prolate aligned $K^\pi=6^-$ state. In this aligned state, the four $N=2$ neutrons couple to $I=K=4$ $(5/2+3/2+1/2+{}^-1/2)$. Figure 5 illustrates why such a configuration is favored energetically. Here we display single-particle Routhians calculated as functions of ϵ and ω/ω_0 for a Nilsson potential cranked around its symmetry axis. As the quadrupole deformation destroys the degeneracy at spherical shape by splitting up orbitals, the nuclear rotation provides its own splitting which can counteract that due to deformation, with the result that bunches of orbitals exist over a range of ϵ values [15]. This effect is more pronounced on the prolate side and for high j subshells, as can be seen

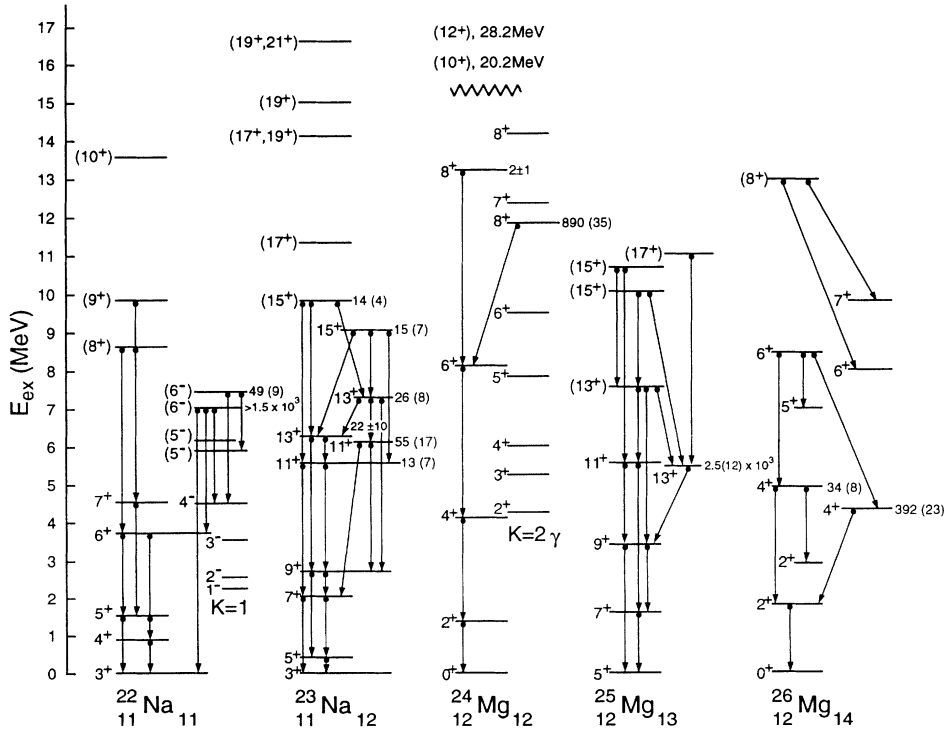

FIG. 3. Partial level schemes for ^{22,23}Na and $^{24-26}$Mg including the complete yrast sequence and the proposed rotational isomers. Measured lifetimes of the isomers in femtoseconds (with uncertainties in parentheses) are listed to the right of each level, and gamma decays from these levels and from all yrast band members are given. The two 5^- states in ^{22}Na and the two $15/2^+$ states in ^{23}Na (the second is more tentative) are also shown as they are included in our discussion. Spins of levels in ^{23}Na and ^{25}Mg are labeled as $2I$.

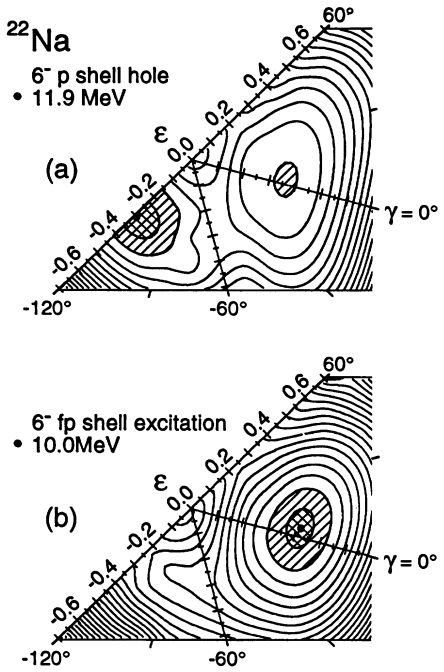

FIG. 4. (a) Calculated potential energy surface (PES) for a one-neutron p-shell hole in ^{22}Na. The configuration is specified as one unpaired N =1 neutron with α=1/2 coupled to two N =2 neutrons also with α=1/2; two N =2 neutrons with α= −1/2; one N =2 proton with α=1/2; two N=2 protons with α=−1/2. The contour line spacing is 1 MeV. The minimum energy relative to the calculated 3^+ ground state is represented by a dot. The minimum along $\gamma = -120°$, with configuration ν[211]3/2 [202]5/2 [101]1/2 ⊗ π[211]3/2, corresponds to the experimental state at 6.958 MeV, while the secondary minimum along $\gamma = 0°$ represents the 7.413 MeV state. (b) Same as (a) but for a one-proton fp-shell excitation. Note the absence in (b) of any bandhead along $\gamma = -120°$ that would compete with the collective minimum at 10.0 MeV calculated excitation energy.

in the $d_{5/2}$ orbitals with positive cranking axis projection. A resulting energy gap appears for particle number 12. Proposed low lying rotational isomers for Na and Mg nuclei are presented as occupied orbitals for each nucleus in which they occur. At the far right is the 6^- state in ^{22}Na. At even larger deformations, a hole in the [101]−3/2 orbital would suggest a relatively low lying K^π=7^- state. Returning to Fig. 4(a), at $\epsilon \sim 0.36$ but near γ=0° and roughly 400 keV higher we see a secondary, collective minimum. The bandhead for this 6^- state corresponds experimentally to the K^π=1^- state at 2212 keV. Comparing the deformation of the collective minimum with that of the shell model (SM), Vermeer obtains $Q_0(6_2^-) = +37.0\ e\,\mathrm{fm}^2$ (theory) and $\pm 38.8\ e\,\mathrm{fm}^2$ from the experimental $B(E2)$ value for the $6_2^- \rightarrow 4_1^-$ transition, which yields $\epsilon \sim 0.32$–0.33 using the relation $Q_0 = (4/5)\ ZA^{2/3}\ r_0^2\ \epsilon(1+\epsilon/2)$ (with r_0=1.2), similar to our result. Vermeer calculates $Q_0(6_1^-) = +38.5\ e\,\mathrm{fm}^2$ using $K = 6$ which yields $\epsilon(6_1^-) \sim 0.33$, again close to our value, and to the 6_2^- value. Experimental studies have derived average $\mid Q_0 \mid$ values from the $B(E2)$ for $4^- \rightarrow 2^-$ and $3^- \rightarrow 1^-$ (K^π=1^-) decays which yield ϵ (K^π=1^- band) = 0.53 ± 0.08 [12] and 0.57 ± 0.03 [13], significantly larger than both the K^π=3^+ ground state band ($\epsilon \sim 0.4$), the tentative K^π=6^- state, and the 6^- member of the K^π=1^- band. Our calculated deformations for $I < 6$ in the (π, α)=$(-, \pm)$ p-shell hole bands are all in the range 0.37–0.41. The reduction in deformation at higher spins in the K^π=1^- band indicates an onset of band mixing and the approach to termination for this band in ^{22}Na.

As is the case in $^{24-26}$Mg, if $K(6_1^-) = 6$, then the $6_1^- \rightarrow 4_1^-$ decay (ΔK=5) along with its short lifetime violates the K selection rule. This violation has been explained by large amounts of Coriolis mixing between different K bands. Alternatively, a more recent explanation to account for a ΔK=25 decay in ^{182}Os proposes tunneling through the γ barrier from −120° to 0° (a prolate

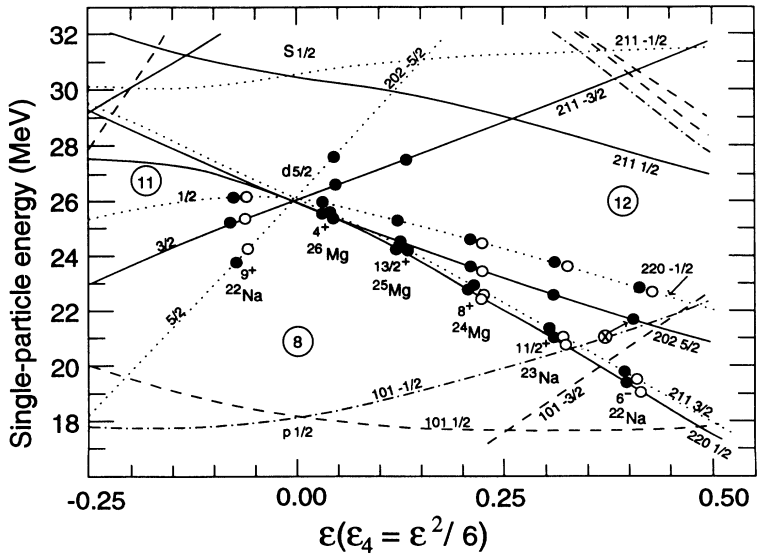

FIG. 5. Single-particle Routhians in the sd shell for a Nilsson potential cranked around its symmetry axis, plotted against ϵ and equivalently ω/ω_0. Encircled numbers represent total particle numbers. Rotational isomers in various nuclei are represented as occupied valence orbitals, with open circles for protons and solid circles for neutrons.

→ oblate → prolate transition) via pairing fluctuations in that nucleus [16]. The single-particle–collective hindrances between individual states in the $A = 20$–26 mass region do not seem to be very strong; lifetimes do not exceed 10^{-11} sec for *sd*-shell isomers (see Fig. 3) compared to the rare earth region where lifetimes can be years (e.g., ^{178}Hf, $K^\pi=16^+$, 2447 keV, $t_{1/2}$=31 years).

Returning to Fig. 4(b), we observe that for a one-particle *fp*-shell excitation there is no aligned configuration that competes favorably with the collective minimum at E^{exc}=10.0 MeV (relative to the 3^+ ground state) and $(\epsilon, \gamma) = (0.42, 5°)$. The lowest energy along $\gamma = -120°$ for $K^\pi=6^-$ occurs at $\epsilon \sim 0.24$ and E^{exc}=19.1 MeV. As Fig. 5 shows, this state would involve exciting a particle across the shell gap at particle number 12 and hence is not expected to be favored. Furthermore, the fact that the energy becomes lower away from $\gamma = -120°$ indicates the strong Coriolis coupling expected for this configuration.

2. *Signature splitting in the yrast bands*

The amount of signature splitting in the $K^\pi=3^+$ and 1^- bands can be estimated by plotting experimental Routhians E^ω vs $\hbar\omega$ [3]. The difference in energy for α=0 and 1 bands at a given ω represents the signature splitting. The appropriate plot is given in Fig. 6, where it is apparent that, for either of two possible candidates for the $5^-(K = 1)$ member, the negative parity $K^\pi=1^-$ band has significantly less splitting than the ground state $K^\pi=3^+$ band. This result is explained by Vermeer *et al.* [17] by looking at the relative contribution of the $d_{5/2}$ configuration to the wave function of each $K^\pi=3^+$ band member. It is the largest component for each member except 6^+[13] and 8^+, the latter having no contribution because a $T = 0$, $I = 8$ state cannot be made from six $d_{5/2}$ particles. The $d_{5/2}$ contribution is greater for odd than even spins. Since it costs less energy to populate $d_{5/2}$ orbitals, the odd spin sequence is shifted down relative to a smooth $I(I + 1)$ dependence. Perhaps the explanation for the oscillation in $d_{5/2}$ components comes from the $K^\pi=0^+$ band as it affects the $K^\pi=3^+$ sequence. $K^\pi=0^+$ bands in odd-odd nuclei have the odd and even spin sequences shifted relative to one another, the so-called Newby shift, due to the residual interaction between the odd proton and neutron. In ^{22}Na, the concept of Newby shifting has not been mentioned in experimental papers because of the convention to treat the $T = 1$, even spin sequence for the $K^\pi=0^+$, [211]3/2−[211]3/2 band as a different band than the $T = 0$, odd spin sequence. However, Freeman *et al.* [12] have placed the two sequences together because of strong $M1$ decays connecting them while Frisk [18] has determined an empirical rule for the sign of the Newby shift E_N and has included ^{22}Na in his discussion, calculating $E_N(^{22}\text{Na}) = -253$ keV. It has been shown in the rare earth region [19] that this shifting of levels can affect other rotational bands in the nucleus even with ΔK up to 4, through higher order Coriolis coupling. In ^{22}Na such coupling between the $K^\pi=0^+$ band and $K^\pi=3^+$ ground state band could explain the signature splitting in the latter.

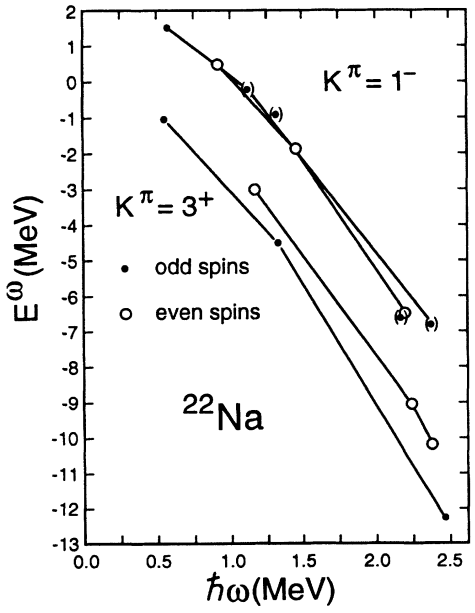

FIG. 6. Experimental Routhians as a function of rotational frequency for the 3^+ ground state band and the 1^- yrast negative parity band in ^{22}Na. In the 1^- band there are two candidates for $I = 5$ and so both have been used to determine data points for comparison. Solid circles represent the odd spin sequence and open circles the even spin sequence.

3. *Band terminations in the mass 20–26 region: ^{22}Na*

For our purposes a band termination is described as a state having the maximum possible spin for the configuration in which the band begins. This implies that such a band can be followed, in some smoothly changing way in plots of spin vs energy and spin vs deformation, up to the termination, but in practice the concept of termination is used even when the trend is not so smooth. Also, it is possible to define a configuration according to the occupation of subshells or alternately according to the occupation of N shells. In the present calculations, the former definition is only approximate while the occupation of (rotating) N shells is unambiguous. For example, in ^{22}Na the $(d_{5/2})^3$ $(d_{5/2})^3$ configuration is rather well defined having a maximum spin of 9^+ while the unambiguously defined $(N=2)^3$ $(N=2)^3$ configuration has a maximum spin of 11^+. Which definition is more proper when comparing with experiment depends on how the energies vary with spin.

To illustrate how different bands terminate, we have plotted in Figs. 7(a,b) the quantity E^{exc} - $\hbar^2/2\Im$ $I(I+1)$ vs I for yrast bands in ^{20}Ne, ^{22}Na (positive and negative parity), and ^{24}Mg. The moment of inertia parameter is chosen according to an average trend for rigid rotation, $\hbar^2/2\Im = 32.3\ A^{-5/3}$ [20]. For the 0^+ ground state band in ^{24}Mg, the maximum spin for eight *sd*-shell particles, 12, has tentatively been observed [21] (see Fig. 3). Figure 7(a) shows that this 12^+ state, encircled to illustrate its aligned nature, is however not favored energetically in

the experimental spectrum. This is consistent with the CNSM calculations which predict that the strongly deformed ($\epsilon \sim 0.48$) configuration $([211]3/2)^{-2}$ $([330]1/2)^2$ (in which two particles in the *sd* shell have been promoted to the *fp* shell) is slightly lower in energy for $I \leq 12$ than the oblate-terminating ground band configuration with eight $N=2$ particles. It has been shown that for nuclei such as ^{24}Mg in the middle of a shell, the dependence of orbital energies on γ as ω increases is such that the total deformation energy of the nucleus does not favor oblate shapes [20].

If a terminating aligned state is favored energetically, it will be from the same kind of shell effects as discussed above for prolate rotational isomers. The curve E-$E_{\rm rot}$ vs increasing I would then be down sloping as the curvature becomes negative. Also, an irregular structure among the data points for a band indicates that small collectivity is present and that shell effects are changing rapidly with angular momentum [20]. At the beginning of a shell oblate-terminating configurations are favored, as the curve for ^{20}Ne in Fig. 7(a) clearly demonstrates. The 8_1^+ level lies at 11.99 MeV excitation, well below the average rotor behavior.

The 3^+ ground state band in ^{22}Na in Fig. 7(a) shows an energy staggering and a low lying 9^+ state which corresponds to the oblate aligned configuration $([202]5/2\ [202]3/2\ [200]1/2)^2_{9+}$ (see Fig. 5). Figure 8 shows the PES for 9^+ with the configuration $\pi(N{=}2)^3$, $\alpha{=}1/2$, $\nu(N{=}2)^3$, $\alpha{=}1/2$, i.e., with six *sd*-shell particles coupled to $\alpha_{\rm tot}{=}1$ corresponding to odd spins. This is the terminating state for this configuration because for $\alpha{=}1/2$, $I = 1/2, 5/2, 9/2$, etc., for both the odd π and ν, and since three like particles (in $d_{5/2}$) can couple to a maximum spin of 9/2, only 9^+ can result. The minimum is only slightly deformed at $\epsilon{=}0.09$, and while the interpolation sets the minimum somewhat away from $\gamma{=}60°$ the softness towards oblate shape is obvious. The predicted energy of 10.5 MeV is only 0.7 MeV away from the experimental value at 9813 keV [17]. The $9_1^+ \rightarrow 7_1^+$ experimental transition strength has not been reported, but the lifetime is estimated at 13±8 fs [17]. The shell model predicts the $E2$ strength to be 7.8 W.u. compared to experimental strengths for the $7 \rightarrow 5$, $6 \rightarrow 4$, and $5 \rightarrow 3$ decays of 17±6, 8.2±0.8, and 4.4±0.6 W.u., respectively [13].

The tentatively assigned 10_1^+, 13.58 MeV level [22] in ^{22}Na also becomes low in Fig. 7(a), contrary to the CNSM prediction. Its calculated parameters are $(\epsilon, \gamma) = (0.19, 45°)$, essentially an oblate aligned state where one nucleon is promoted from $(d_{5/2})_{1/2}$ to $(d_{3/2})_{3/2}$ relative to the 9_1^+ level. The inclusion of higher orbitals in the 10_1^+ wave function in contrast with the pure $d_{5/2}$, 9_1^+ configuration can explain why the 10^+ state is not favored in the calculations. The discrepancy between theory and experiment for $I = 10$ is unexpectedly high and suggests

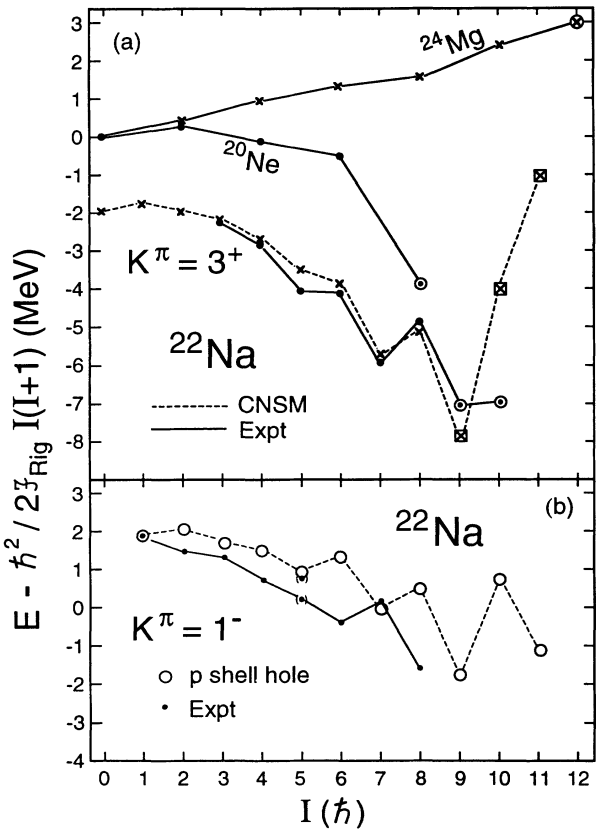

FIG. 7. Theory and experiment are compared for the total energy minus an average liquid drop contribution for (a) the $K^\pi{=}3^+$ band in ^{22}Na, the yrast band in ^{20}Ne (solid dots), and the yrast band in ^{24}Mg (×); and (b) the experimental $K^\pi{=}1^-$ band in ^{22}Na along with the calculated yrast *p*-shell hole band. Terminating states are labeled as ⊙ (expt) and □ (CNSM). We have used $\hbar^2/2\Im{=}32.3A^{-5/3}$. The calculated curve for $K^\pi{=}3^+$ in (a) extends to $I = 0$ because the CNSM predicts the $K^\pi{=}0^+$ band as yrast and hence cannot generate a $K^\pi{=}3^+$ sequence. Experiment and theory are normalized at $I{=}3$. In (b), the staggering predicted for the *p*-shell band is opposite to that of experiment; i.e., the favored signature is calculated to be for odd spins, not even, although the observed staggering is small. Both experimental candidates for the 5^- member of this band are included for comparison; we have followed the sequence of Ref. [5].

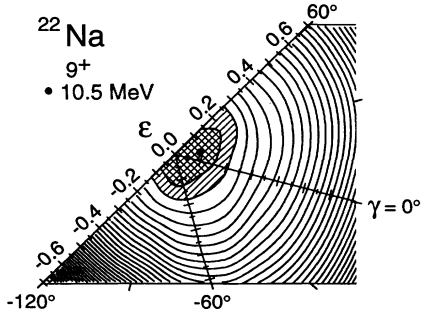

FIG. 8. The 9^+ PES's for fixed configuration $\pi(N = 2)^3$ $\nu(N = 2)^3$, $\alpha_{\rm tot}{=}1$ in ^{22}Na (see Fig. 5) with $(\epsilon_2,\gamma) = (0.09, 14°)$. This is the terminating state for such a configuration and hence only one minimum will be present.

further experiments to obtain a more certain spin assignment for the observed 13.58 MeV state.

The 11_1^+ state is predicted to lie at 25.2 MeV with $(\epsilon, \gamma) = (0.19, 60°)$. This is the maximum *sd*-shell spin for six particles. Even more than for the 12^+ state in ^{24}Mg, this aligned state is predicted to be energetically unfavored. The yrast 11^+ state is predicted to lie 2.9 MeV lower at deformation $(\epsilon, \gamma) = (0.46, 11°)$, corresponding to a 1π, 1ν *fp*-shell excitation.

In Fig. 7(b) we plot the experimental $K^\pi=1^-$ band in ^{22}Na (solid circles) along with the lowest calculated *p*-shell proton hole band (open circles). We have normalized the energy of the calculated band to that of experiment. The $\alpha=1$ sequence of the $K^\pi=1^-$ band is predicted to terminate at $I = 11$ with $(E^{\rm exc},\epsilon,\gamma) = (22$ MeV, 0.23, 60°) while the $\alpha=0$ sequence should terminate at $I = 12$ with $E^{\rm exc} \sim 35$ MeV [not shown in Fig. 7(b)]. Although the observed staggering between favored and unfavored signatures is small for this band, it is opposite to that predicted by the CNSM. If the experimental consensus is correct regarding the *p*-shell nature of this band, such a signature inversion that continues possibly up to the band termination has not been seen before and we do not have an explanation for this behavior. Already by spin 4 the band built on the lowest *fp*-shell excitation is calculated to be favored energetically over the *p*-shell hole configuration.

B. ^{23}Na

1. The $11/2^+$ levels at 5533 keV and 6117 keV

As Fig. 3 shows, the positive parity levels in ^{23}Na have been tentatively identified up to $I = 21/2$, including several candidates for $I = 15/2$–$21/2$ [23–25]. Gamma decays relevant to our discussion are shown in Fig. 3; no decay has been seen for proposed $I \geq 17/2$. The 5533 keV state has been established to have $I^\pi=11/2^+$ (although not unambiguously), and is generally accepted as belonging in the $K^\pi=3/2^+$ ground state band [25–27] with an $11/2^+ \rightarrow 7/2^+$ transition strength of 7^{+14}_{-3} W.u.

A level at 6117 keV (5/2–11/2) has also been tentatively assigned $11/2^+$, based on its decay to the $9/2_1^+$ and $7/2_1^+$ ground band members [5, 28] and based on decay from tentative $15/2^+$ states into it [29]. This $11/2_2^+$ state was first suggested as having $K^\pi=11/2^+$ by Cole *et al.* [30] using the shell model and again by Guttormsen *et al.* [31] using the particle-rotor model without pairing. The latter group proposed the configuration $\pi[211]3/2\ \nu[211]3/2\ [202]5/2$, i.e., a one-neutron excitation from [211]3/2 to [202]5/2 (see Fig. 2). However, three (quasi) particle states were not considered explicitly in the particle-rotor analysis of ^{23}Na; i.e., no calculated $K^\pi=11/2^+$ state was presented. Instead, their suggestion of $K^\pi=11/2^+$ along with 13/2 and 15/2 band members at 7.27 MeV and 9.04 MeV, respectively, came from analyzing the experimental work of Thornton *et al.* [25]. Vermeer [5] suggested $K^\pi=11/2^+$ for the 6117 keV state based on its relation to the $11/2_1^+$ state being similar to that of 6_1^- vs 6_2^- in ^{22}Na. The 6117 $\rightarrow$ 2076 ($11/2 \rightarrow 7/2$) transition has $B(E2)_{\rm expt} = 0.44 \pm 0.16$ W.u. (7 W.u. for $11/2_1^+ \rightarrow 7/2_1^+$), indicating a different structure for $11/2_2$ than for $11/2_1$. The shell model predicts that, as with the 6_1^- level, there is a large $d_{5/2}$ component for the $11/2_2^+$ wave function [>30% $(d_{5/2})^7$] while less than 10% of the $11/2_1^+$ wave function is $(d_{5/2})^7$ [5].

Figure 9(a) illustrates the PES for $11/2^+$ configurations in ^{23}Na based on the odd proton having $\alpha_\pi = -1/2$. The yrast state calculated at $E^{\rm exc} = 5.4$ MeV is a $K^\pi=11/2^+$ bandhead with $(\epsilon, \gamma) = (0.26, -120°)$. A collective minimum can be seen approximately 0.5 MeV higher at 5.9 MeV (expt. 5.53 MeV) with $(\epsilon, \gamma) = (0.32, 0°)$, slightly more deformed than the $K^\pi=11/2^+$ min-

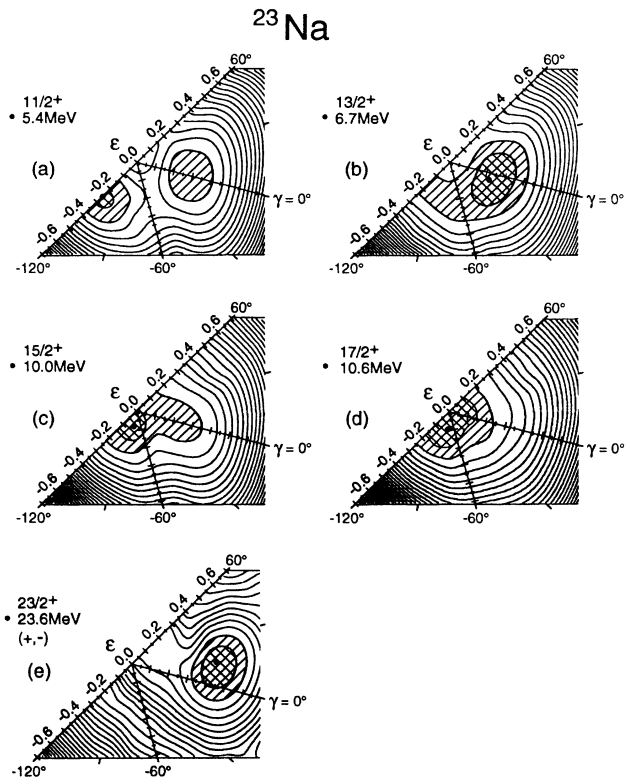

FIG. 9. Selected PES's for ^{23}Na drawn in the same way as for ^{22}Na in Fig. 4. The diagrams represent fixed configurations for (a) $11/2^+$, (b) $13/2^+$, (c) $15/2^+$, and (d) $17/2^+$. Two $N = 2$ neutrons are placed in $\alpha_\nu=1/2$ and two in $\alpha_\nu=-1/2$. Similarly, there are two (one) protons in $\alpha_\pi=1/2$ and one (two) protons in $\alpha_\pi=-1/2$ for $I = 13/2, 17/2$ (I=11/2, 15/2), respectively. In (e), the $23/2^+$ surface represents yrast configurations. In the $11/2^+$ PES, minima along $\gamma = -120°$ and 0° correspond experimentally to the 6117 keV and 5533 keV states, respectively. In the $13/2^+$ PES, the minimum along $\gamma = -120°$ at $\epsilon\sim0.17$ is roughly 1.6 MeV higher than the absolute minimum (1.04 MeV higher in experiment). The $15/2^+$ absolute minimum at $(\epsilon,\gamma) = (0.09, -82°)$ is a mixture of two aligned, essentially spherical $d_{5/2}$ states. For $17/2^+$, the minimum is again nearly spherical and represents an aligned configuration. In the $23/2^+$ PES, the maximum *sd*-shell spin for seven particles is an oblate local minimum along $\gamma=60°$ with $\epsilon\sim0.15$ and $E^{\rm exc}=26.2$ MeV. The absolute minimum has $(\epsilon,\gamma) = (0.46, 15°)$ and corresponds to a one-π, one-ν *fp*-shell excitation.

imum and built on the $K^\pi=3/2^+$ ground state which is predicted to start at $\epsilon \sim 0.35$. Thus, the calculated $11/2^+_{1,2}$ levels are within 0.7 MeV of experiment which is quite reasonable although their order is inverted. The shell model predicts the $11/2^+_{1,2}$ levels to lie at 5.391 MeV and 6.149 MeV [5], very close to experiment, with Q_0 (SM) values that yield $\epsilon(11/2_1,\ K^\pi=3/2^+)\sim 0.36$ (CNSM=0.32) and $\epsilon(K^\pi=11/2^+)\sim 0.37$ (CNSM=0.26). For the latter state this is an unusually large discrepancy between the two models. One reason for this discrepancy might be the assumption of pure K in the projection formula

$$Q_s = \{[3K^2 - I(I+1)]/(I+1)(2I+3)\}Q_0, \qquad (1)$$

translating between the spectroscopic quadrupole moment Q_s calculated in the SM and the static quadrupole moment Q_0.

2. The $13/2^+$ levels at 6237 keV and 7273 keV

A level experimentally observed at 6237 keV has been assigned $K^\pi I=3/2^+$, 13/2 based on its energy and decay properties [26,28,29]. It has a $B(E2)$ transition probability to the $9/2^+_1$ state of 60±27 W.u. [29] (SM = 38.7 [29], 43.9 [30]). The $13/2^+$ member of the next positive parity band, $K^\pi=1/2^+$, has been tentatively assigned near 10.0 MeV [24, 25] and alternatively at 10.9 MeV [23]. In between 6.2 and 10 MeV there are two more tentative $13/2^+$ states, at 7.27 and (more tentative) at 8.32 MeV [24, 25, 29].

The $13/2^+$, 7.27 MeV state decays to $9/2^+_1$ with a $B(E2)$ of only 8.4±2.7 W.u. (in contrast with 60±27 W.u. for $13/2_1 \rightarrow 9/2_1$); other decays are 36% to $11/2^+_2$ and 11% to $13/2^+_1$ [29]. In Fig. 9(b) we display the PES for $13/2^+$ configurations in ^{23}Na, where the absolute minimum is at $E^{\rm exc} = 6.7$ MeV with $(\epsilon,\gamma) = (0.23, -8°)$ corresponding to the experimental $K^\pi=3/2$ band member at 6.24 MeV. A secondary minimum appears along $\gamma = -120°$ with $\epsilon \sim 0.17$ and $E^{\rm exc} \sim 8.2$ MeV, roughly 1.6 MeV above the collective minimum, in comparison with the experimental difference of 1.03 MeV between the lowest two $13/2^+$ states. This aligned state along $\gamma = -120°$ corresponds to $K^\pi=13/2^+$ and the $(d_{5/2})^7$ configuration π [202]5/2 ν [202]5/2 [211]3/2. Figure 5 shows the energy stability for such a configuration that consists of down-sloping prolate valence orbitals. Moving the proton from [211]3/2 in the illustrated $11/2^+$ configuration to [202]5/2 generates the $K^\pi=13/2^+$ bandhead. A second possible $K^\pi=13/2^+$ state can result from the Nilsson configuration π[211]3/2 ν[220]1/2 [211]3/2 [202]5/2 [211]1/2, i.e., a two-ν excitation mixing $d_{5/2}$ with the $s_{1/2}$ subshell and five unpaired nucleons. A more detailed study shows that it is the $(d_{5/2})^7$ configuration which is lowest. The configuration with one neutron in $s_{1/2}$ comes out as essentially spherical approximately 1.5 MeV higher in energy. If, as we propose, the 7.27 MeV state has $K^\pi=13/2^+$ or at least contains large admixtures of this K value, the decay to $K^\pi=11/2^+$ at 6117 keV provides a K-allowed deexcitation mode, while the decay to $13/2_1$ and $9/2_1$ is consistent with all other proposed isomeric transitions in Na and Mg nuclei in that large K admixtures are present and the use of K as a valid quantum number at high spin is only an ideal concept for nuclei in this region.

3. The levels at 9.04 and 9.80 MeV

A comparison of the experimental members of the $K^\pi=3/2^+$ band with the CNSM and SM calculations is presented in Fig. 10 with the energy axis chosen in such a way as to emphasize deviations from $I(I+1)$ (see Fig. 7 and the explanation above for ^{22}Na). Energy systematics suggest $E(15/2^+,\ K=3/2) \sim$ 10–10.5 MeV. Experimentally the $15/2^+_1$ level is unanimously assigned at 9041 keV, while the spin of the level at 9802 keV has been assigned as $15/2^+$ [24, 25, 29] and unassigned K value, and alternatively as $17/2^+$ [23, 32–34]. These latter authors also consider the 9041 keV and 9802 keV levels to be the 15/2 and 17/2 members of the $K^\pi=3/2^+$ ground state band. The experimental spin uncertainty of the 9802 keV level hinges on whether or not there is a decay of the 9802 keV state to the $11/2^+_1$ state [29]. SM calculations of Wildenthal (referenced in [24]) and Cole *et al.* [30] favor the $15/2^+$ assignment for 9802 keV, with calculated energies (MeV) for $15/2_1$, $15/2_2$ of 9.06, 9.81 [24] and 9.08, 9.86 [30]. Wildenthal also calculates $E(17/2^+_1) = 10.92$ MeV. Cole *et al.* [30] place $15/2_1$ into the $K^\pi=3/2^+$ band, while Guttormsen *et al.* [31] using the particle-rotor model place the 9.80 MeV

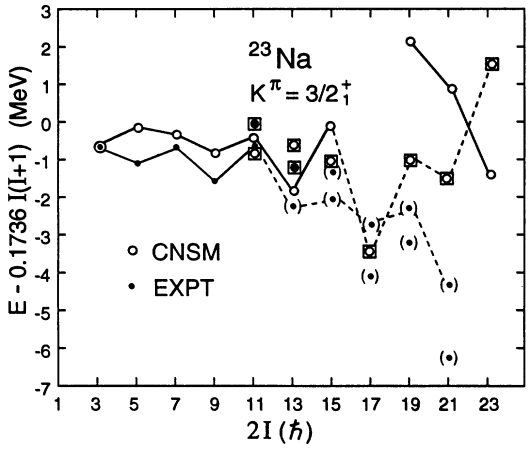

FIG. 10. Same as for Fig. 7 but for the $3/2^+$ band and the yrast sequence of spins in ^{23}Na. Also, for $I \geq 19/2$, we display the lowest positive parity band built on a one-π, one-ν fp-shell excitation that becomes yrast at I=23/2. For I = 11/2–15/2, we plot both for experiment and theory the two lowest lying states of each spin, with aligned configurations enclosed in squares. Dashed lines between states for $I > 11/2$ (expt) and $I > 15/2$ (CNSM) indicate that beyond these respective spins, levels cannot be grouped into separate bands. In the CNSM curve, dashed lines are shown to guide the eye and are not meant to suggest members of the yrast band. For I between 17/2 and 21/2, there are two alternatives proposed experimentally for the yrast state and both are included here. The states closer in energy to SM predictions are connected by the dashed line.

level into this band as $15/2_2$. However, both studies proposed that the $I = 15/2$ strengths of the $K^\pi=3/2^+$ band and a $K^\pi=11/2^+$ band starting at 6117 keV (see Sec. III B 1 above on the $K^\pi=11/2^+$ state) are divided between the two levels. This $K^\pi=11/2^+$ band, with a proposed 13/2 member at 7.27 MeV (our proposed $K^\pi=13/2^+$ state) would have a rotational parameter of slightly above 100 keV [31], or roughly half of that for lower lying bands. This implies a much larger deformation for the $K^\pi=11/2^+$ band than for $K^\pi=3/2^+$, but the CNSM predicts the opposite to be true (see above for discussion of ϵ values) while the SM predicts ϵ values similar to the CNSM.

Figure 9(c) illustrates $15/2^+$ states in ^{23}Na. The minimum at $E^{\rm exc}$=10.1 MeV (expt. 9.04 MeV) with $(\epsilon,\ \gamma) = (0.09,\ -\ 82°)$ corresponds to a mixture of two states. However, both components of the admixture are $K^\pi=15/2^+$ aligned configurations, calculated as pure $d_{5/2}$ and essentially spherical. The lowest collective $15/2^+$ state is calculated to lie 1.0 MeV above this minimum, with $\epsilon,\gamma = 0.2,\ 7°$. The experimental (SM) $B(E2)$ values for $15/2_1^+ \rightarrow 11/2_1^+$ and $15/2_2^+ \rightarrow 11/2_1^+$ are $20\pm^{10}_{12}$ (42) and 10 ± 5 (13) [29,30] which indicate similar collectivity in the $15/2^+$ levels. Clearly, the experimental evidence does not dictate assigning $K^\pi=15/2^+$ to either of the proposed $15/2^+$ states. We can, however, compare this situation with that of the $11/2^+$ and $13/2^+$ states discussed above where the competing collective and single-particle configurations have $\Delta E_{\rm expt}$ = 584 keV (11/2) and 1036 keV (13/2). For $15/2^+$ we have $\Delta E_{\rm expt}$ = 761 keV and $\Delta E_{\rm CNSM}$ = 1.0 MeV with $15/2_1^+$ calculated as $K^\pi=15/2^+$. The model again predicts an interplay between aligned and collective states, where the former is now close to spherical, and the data suggest a highly admixed situation, even more so than for 11/2 or 13/2, and not, however, an admixture of $15/2^+$ members of $K^\pi=11/2^+$ and $3/2^+$ bands as proposed earlier [30, 31].

4. Band Terminations in ^{23}Na

a. Proposed $17/2^+$ levels. The highest possible spin for a $(d_{5/2})^7$ arrangement in ^{23}Na is $17/2^+$. Analogous to the $K^\pi=13/2^+$ situation discussed above, Fig. 5 illustrates the energy stability for a $K^\pi=17/2^+$ level with configuration π [202]5/2 [211]3/2 [220]1/2 ν [202]5/2 [211]3/2 [220]1/2 [220]$^-$1/2. Figure 9(d) presents the $17/2^+$ PES, where we see a broad minimum at 10.6 MeV excitation with $\epsilon,\gamma = 0.1,\ -76°$. Although the absolute minimum is away from $-120°$, this is the $K^\pi=17/2^+$ state, calculated as nearly spherical again which is a trademark of $d_{5/2}$ subshell condensates in *sd*-shell nuclei.

Experimentally, the $17/2_1^+$ level is proposed either at 9.81 MeV [23, 32–34] (see above, Sec. III B 3) or at 11.29 MeV [23–25]. The 11.29 MeV state has been proposed as $K^\pi I = 3/2^+17/2$ based on energy systematics alone [24, 25] and on calculated $B(E2)$ values [27, 30]; no gamma decay has been seen from this state. Thornton *et al.* [25] also suggest the next $17/2^+$ state to lie at 11.55 MeV. The SM predicts $E(17/2_{1,2}^+)$ = 10.92, 11.58 MeV [24, 27] while the particle-rotor model calculates $E(17/2_1^+)$ = 11.0 MeV.

The experimental picture is not clear enough yet for $I > 15/2$ to make a detailed comparison with theory. We can say that the CNSM predicts low lying states of single-particle nature for spins from $11/2^+$ to $17/2^+$, and the experimental and theoretical evidence for mixing between proposed $K = I$ states and collective states of the same spin, built on lower K bandheads, indicates that grouping levels into rotational bands is not a valid procedure beyond $I^\pi=11/2^+$ in this nucleus. In Fig. 10 we indicate by a dashed line for experiment this breakdown in band structure. For the CNSM curve, dashed lines connect yrast states beyond $I = 15/2$, not to suggest $3/2^+$ band members, but rather to guide the eye. Also displayed are the proposed rotational isomers for I=11/2–15/2, for both experiment and theory.

b. States with $I^\pi \geq 19/2^+$. The next fully aligned *sd*-shell spin in ^{23}Na beyond 17/2 (keeping particles in lowest energy orbitals) is 19/2, corresponding to $(d_{5/2})^6$ $(s_{1/2})^1$, i.e., one-half unit more of spin added to the 9^+, ^{22}Na band termination discussed earlier, but also mixing in a higher energy subshell. Promoting one particle from $(s_{1/2})$ in the above 19/2 configuration to $(d_{3/2})_{3/2}$ can generate a $21/2^+$ state and promoting one particle each from $s_{1/2}$ and $(d_{5/2})_{1/2}$ into $(d_{3/2})_{3/2}$ generates a $23/2^+$ aligned state, with 23/2 as the maximum possible *sd*-shell spin for seven nucleons. Thus the level scheme for ^{23}Na beyond $I = 15/2$ should make an essentially complete change from collective to single-particle behavior, and the jagged curve in Fig. 10 bears this out where we have plotted both of the two possible experimental candidates for yrast levels with spins $17/2^+ \leq I \leq 21/2^+$ and connected those levels best reproduced by SM calculations. The SM predicts the $K^\pi=3^+$ band to remain yrast through to the termination, but of course this model did not allow for particle hole excitations outside the *sd* shell. The fact that this single-particle nature exists in an experimentally obtainable region of spins is very rare and offers a good possibility for more detailed study of these levels. With the availability of large gamma detector arrays, it should be possible to detect gamma decay from these high spin states and perhaps obtain information on lifetimes, $B(E2)$ values, and deformation.

The total PES (including all possible configurations) for $23/2^+$ states in ^{23}Na is shown in Fig. 9(e). The termination of the *sd* shell gives an oblate configuration with $(E,\epsilon,\gamma) \sim$ (26.2 MeV, 0.15, 60°), roughly 2.6 MeV above the absolute minimum. This latter yrast configuration is calculated to be triaxial with (ϵ,γ) = (0.46, 15°) corresponding to a one-π, one-ν *fp*-shell excitation. Figure 10 illustrates the band crossing at spin 23/2.

5. Band terminations in other sd-shell nuclei

Table I reviews the current status of maximum spins reached in selected nuclei from ^{20}Ne to ^{26}Mg, including the maximum *sd*-shell spin for that nucleus (which may be higher than the ground band termination), and the estimated ground state quadrupole deformation. The ϵ

TABLE I. Review of experimental results for prolate deformed nuclei in the first half of the *sd* shell where band terminations have been approached or reached. Values for ϵ are calculated from the intrinsic quadrupole moment Q_0 as $Q_0 = 4/5\ ZA^{2/3}r_0^2\ \epsilon(1+\epsilon/2)$ with r_0=1.2 fm and Q_0 taken from the references listed in the footnotes. The maximum *sd*-shell spin may or may not correspond to the ground state band termination; in ^{22}Na, for example, the ground state band terminates at 9^+.

	Nucleus							
	^{20}Ne	^{21}Ne	^{22}Ne	^{22}Na	^{23}Na	^{24}Mg	^{25}Mg	^{26}Mg
ϵ[a]	0.54	0.43	0.43	0.4	0.43	0.46	0.40	0.39
Maximum *sd*-shell spin	8	19/2	10	11	23/2	12	25/2	13
Highest observed spin[b]	8	(17/2)	10	(10)	(21/2)	(12)	(17/2)	(8)

[a] ϵ for even-even nuclei taken from $2_1^+ \rightarrow 0_1^+$ transition in Ref. [27], ^{21}Ne ground state from Ref. [35], ^{22}Na from $4_1^+ \rightarrow 3_1^+$ transition in Ref. [12], ^{23}Na ground state from Ref. [36], ^{25}Mg ground state from Ref. [3].
[b] ^{20}Ne [37], ^{21}Ne [38], ^{22}Ne [39], ^{22}Na [22], ^{23}Na [23–25], ^{24}Mg [21], ^{25}Mg [3], ^{26}Mg [40].

values are derived either from Q_0 for the ground state or from the $B(E2)$ for the decay of the first excited state. The five nuclei to the right also contain examples of prolate rotational isomers, while ^{25}Mg may contain an oblate $K^\pi=11/2^+$ bandhead [3].

Two distinct features are evident from Table I. The first is the large values of deformation for each nucleus. The second is that $I^{\max}$ or $(I^{\max}-1)$ has tentatively been reached in six of the eight nuclei listed. The few band terminations observed in the rare earth region have only recently been approached due to improved detector technologies, while the 8^+ ^{20}Ne termination has been known since 1966. No attempts have been published yet using large gamma detector arrays to investigate the *sd*-shell region and we feel that, especially if particle-gamma or particle-gamma-gamma coincidence methods are used, much new information on the level schemes at high spin can be obtained.

IV. CONCLUSION

In ^{22}Na and ^{23}Na as in Mg nuclei the concept of rotational isomerism provides an explanation for certain low lying high spin states in terms of rotation-induced shell effects. On the other hand, the relatively short half-lives and gamma decay between these isomers and lower lying states show that one cannot view these prolate states as either purely aligned or collective. Rather the intrinsic structure underlying high spin states in Mg and Na nuclei is complex and requires a more complete search for gamma decay properties in order to be fully understood. Using the CNSM we have given theoretical support for several low lying high spin states in ^{22,23}Na as consisting of primarily single-particle character. In the limit of pure K values, we can assign these states as having $I = K$. Specifically, in ^{22}Na they are 6_1^- at 6.958 MeV and 9_1^+ at 9.813 MeV; in ^{23}Na they are $11/2_2^+$ at 6.117 MeV, $13/2_2^+$ at 7.273 MeV, $15/2^+$ at 9.041 or 9.802 MeV, and a calculated $17/2^+$ state at 10.6 MeV with highly tentative experimental candidates either at 9.802 or 11.55 MeV.

Because of the relatively large frequencies of rotation that can be reached in deformed *sd*-shell nuclei compared to heavier mass regions where the bulk of high spin spectroscopy has been performed, and because the *sd* shell is small enough in particle number to allow shell model and cluster model calculations to be performed, this mass region provides an excellent opportunity to study nuclear structure effects from a variety of view points not possible in other mass regions. The CNSM in its current form as applied to light nuclei does not include pairing or residual *n-p* interaction terms for odd-odd nuclei but is still quite useful in studying the interplay between collective and single-particle effects in these nuclei.

ACKNOWLEDGMENTS

This investigation was supported by the National Science Foundation under Contract No. PHY92-07336 with Florida State University. One of us (I.R.) acknowledges financial support from the Swedish Natural Science Research Council.

[1] I. Ragnarsson and S. Åberg, in *Proceedings of the Nuclear Physics Workshop, I.C.T.P.*, Trieste, Miramare, Italy, 1981, edited by C.H. Dasso (North-Holland, Amsterdam, 1982).
[2] I. Ragnarsson, S. Åberg, and R.K. Sheline, Phys. Scr. **24**, 215 (1981).
[3] D.M. Headly, R.K. Sheline, S.L. Tabor, U.J. Hüttmeier, C.J. Gross, E.F. Moore, B.H. Wildenthal, H.R. Weller, R.M. Whitton, and I. Ragnarsson, Phys. Rev. C **38**, 1698 (1988).
[4] R.K. Sheline, I. Ragnarsson, S. Åberg, and A. Watt, J. Phys. G **14**, 1201 (1988).
[5] W.J. Vermeer, Phys. Lett. B **234**, 219 (1990).
[6] T. Bengtsson and I. Ragnarsson, Nucl. Phys. **A436**, 14 (1985).
[7] G.M. Temmer and N.P. Heydenburg, Phys. Rev. **111**, 1303 (1958).
[8] J.D. Garrett, R. Middleton, and H.T. Fortune, Phys.

Rev. C **4**, 165 (1971).
[9] E. Rivet, R.H. Pehl, J. Cerny, and B.G. Harvey, Phys. Rev. **141**, 1021 (1966).
[10] C.C. Lu, M.S. Zisman, and B.G. Harvey, Phys. Rev. **186**, 1086 (1969).
[11] Y. Kadota, K. Ogino, K. Obori, Y. Taniguchi, T. Tanabe, M. Yasue, and J. Schmizu, Nucl. Phys. **A458**, 523 (1986).
[12] R.M. Freeman, F. Haas, B. Heusch, J. Fernandez Castillo, J.W. Olness, and A. Gallmann, Phys. Rev. C **8**, 2182 (1973).
[13] J.D. MacArthur, A.J. Brown, P.A. Butler, L.L. Green, C.J. Lister, A.N. James, P.J. Nolan, and J.F. Sharpey-Schafer, Can. J. Phys. **54**, 1134 (1976).
[14] J.D. Garrett, H.T. Fortune, and R. Middleton, Phys. Rev. C **4**, 1138 (1971).
[15] I. Ragnarsson, Phys. Lett. **80B**, 4 (1978).
[16] T. Bengtsson, R.A. Broglia, E. Vigezzi, F. Barranco, F. Dönau, and Jing-ye Zhang, Phys. Rev. Lett. **62**, 2448 (1989).
[17] W.J. Vermeer, D.M. Pringle, E.F. Garman, and I.F. Wright, Phys. Lett. B **217**, 28 (1989).
[18] H. Frisk, Z. Phys. A **330**, 241 (1988).
[19] A.K. Jain, J. Kvasil, R.K. Sheline, and R.W. Hoff, Phys. Rev. C **40**, 432 (1989).
[20] I. Ragnarsson, Z. Xing, T. Bengtsson, and M.A. Riley, Phys. Scr. **34**, 651 (1986).
[21] A. Szanto de Toledo, T.M. Cormier, M.M. Coimbra, N. Carlin Filho, P.M. Stwertka, and N.G. Nicolis, Phys. Rev. C **30**, 1706 (1984).
[22] J. Gomez del Campo, J.L.C. Ford, Jr., R.L. Robinson, P.H. Stelson, and S.T. Thornton, Phys. Rev. C **9**, 1258 (1974).
[23] J. Gomez del Campo, D.E. Gustafson, R.L. Robinson, P.H. Stelson, P.D. Miller, J.K. Bair, and J.B. McGrory, Phys. Rev. C **12**, 1247 (1975).
[24] D.E. Gustafson, S.T. Thornton, T.C. Schweizer, J.L.C. Ford, Jr., P.D. Miller, R.L. Robinson, and P.H. Stelson, Phys. Rev. C **13**, 691 (1976).
[25] S.T. Thornton, D.E. Gustafson, K.R. Cordell, L.C. Dennis, T.C. Schweizer, and J.L.C. Ford, Jr., Phys. Rev. C **17**, 576 (1978).
[26] R.A. Lindgren, R.G. Hirko, J.G. Pronko, A.J. Howard, M.W. Sachs, and D.A. Bromley, Nucl. Phys. **A180**, 1 (1972).
[27] M. Carchidi and B.H. Wildenthal, Phys. Rev. C **37**, 1681 (1988).
[28] G.G. Frank, R.V. Elliott, R.H. Spear, and J.A. Kuehner, Can. J. Phys. **51**, 1155 (1973).
[29] G.K. Kekelis, A.H. Lumpkin, K.W. Kemper, and J.D. Fox, Phys. Rev. C **15**, 664 (1977).
[30] B.J. Cole, D. Kelvin, A. Watt, and R.R. Whitehead, J. Phys. G **3**, 919 (1977).
[31] M. Guttormsen, T. Pedersen, J. Rekstad, T. Engeland, E. Osnes, and F. Ingebretsen, Nucl. Phys. **A338**, 141 (1980).
[32] T.M. Cormier, E.R. Cosman, L. Grodzins, Ole Hansen, S. Steadman, K. van Bibber, and G. Young, Nucl. Phys. **A247**, 377 (1975).
[33] P.W. Green, G.D. Jones, D.T. Kelly, J.A. Kuehner, and D.T. Petty, Phys. Rev. C **12**, 887 (1975).
[34] D. Evers, G. Denhöfer, W. Assmann, A. Harasim, P. Konrad, C. Ley, K. Rudolph, and P. Sperr, Z. Phys. A **280**, 287 (1977).
[35] A.J. Howard, J.P. Allen, and D.A. Bromley, Phys. Rev. **139**, B1135 (1965).
[36] P.M. Endt and C. Van der Leun, Nucl. Phys. **A310**, 1 (1978).
[37] J.A. Kuehner and R.W. Ollerhead, Phys. Lett. **20**, 301 (1966).
[38] A. Hoffmann, P. Betz, H. Röpke, and B.H. Wildenthal, Z. Phys. A **332**, 289 (1989).
[39] E.M. Szanto, A. Szanto de Toledo, H. Klapdor, M. Diebel, J. Fleckner, and U. Mosel, Phys. Rev. Lett. **42**, 622 (1979).
[40] F. Glatz, S. Norbert, E. Bitterwolf, A. Burkard, F. Heidinger, Th. Kern, R.Lehmann, H. Röpke, J. Siefert, C. Schneider, and B.H. Wildenthal, Z. Phys. A **324**, 187 (1986).